The Journal of Experimental Biology 209, 3664-3676
Published by The Company of Biologists 2006
doi:10.1242/jeb.02415

Actions of kinin peptides in the stomatogastric ganglion of the crab *Cancer borealis*

Shari R. Saideman[1], Andrew E. Christie[2], Pieter Torfs[3], Jurgen Huybrechts[3], Liliane Schoofs[3] and Michael P. Nusbaum[1,*]

[1]*Department of Neuroscience, University of Pennsylvania School of Medicine, Philadelphia, PA 19104-6074, USA,*
[2]*Department of Biology, University of Washington, Box 351800, Seattle, WA 98195-1800, USA and*
[3]*Laboratory of Developmental Physiology, Genomics and Proteomics, Katholieke Universiteit Leuven, Naamsestraat 59, B-3000 Leuven, Belgium*

*Author for correspondence (e-mail: nusbaum@mail.med.upenn.edu)

Accepted 28 June 2006

Summary

To fully understand neuronal network operation, the influence of all inputs onto that network must be characterized. As in most systems, many neuronal and hormonal pathways influence the multifunctional motor circuits of the crustacean stomatogastric ganglion (STG), but the actions of only some of them are known. Therefore, we characterized the influence of the kinin peptide family on the gastric mill (chewing) and pyloric (filtering of chewed food) motor circuits in the STG of the crab *Cancer borealis*. The kinins are myoactive in arthropods and they occur within the arthropod central nervous system (CNS), but their CNS actions are not well characterized in any species. The pevkinins were first identified in the shrimp *Penaeus vannamei*, but they have yet to be studied in the STG of any species. We identified kinin-like immunolabeling (KLI) in the pericardial organs (POs) in *C. borealis*, but there was no KLI within the STG. The POs are a major source of hormonal influence on the STG. Pevkinin peptides activated the pyloric circuit and they caused a modest increase in the speed of ongoing pyloric rhythms. This modest influence on cycle speed resulted in part from pevkinin excitation of the lateral pyloric neuron, whose strengthened inhibitory synapse onto the pyloric pacemaker neurons limited the pevkinin-mediated increase in cycle speed. The pevkinin excitation of the pyloric rhythm was not strong enough to interfere with the previously documented, gastric mill rhythm-mediated weakening of the pyloric rhythm. Pevkinin also had little influence on the gastric mill rhythm. These results indicate that the kinin peptides have distinct and selective modulatory actions on the pyloric rhythm.

Key words: neuromodulation, central pattern generator, pyloric rhythm, gastric mill rhythm, motor circuits, immunolabeling.

Introduction

Kinin peptides were first isolated from the central nervous system (CNS) of insects, and more recently from mollusks and crustaceans (Torfs et al., 1999). Thus far, the biological actions of these peptides are best documented in peripheral structures, where they are associated with myotropic and diuretic activity (Torfs et al., 1999; Gäde, 2004). The first identified members of this family, the leucokinins (LKs), were isolated from the cockroach *Leucophaea maderae* (Holman et al., 1986). Since then, more than 30 kinin family members have been isolated from many insect species (Holman et al., 1990; Schoofs et al., 1992; Hayes et al., 1994; Veenstra, 1994; Blackburn et al., 1995; Predel et al., 1997; Nieto et al., 1998; Terhzaz et al., 1999). The insect kinins all share the C-terminal amino acid sequence $FX^1X^2WGamide$, where X^1 is F, H, N, S or Y, and X^2 is A, P or S. The non-insect members share this sequence structure but for the terminal amino acid being changed from glycine to serine in lymnokinin (snail) and alanine in some pevkinin (shrimp) family members (Cox et al., 1997; Nieto et al., 1998).

Kinin peptides are likely to act both within the arthropod CNS and as circulating hormones. Supporting the former possibility is the finding that kinin-like immunolabeling (KLI) occurs in the CNS of many arthopods, staining neuronal somata in the supraesophageal (brain), subesophageal, thoracic and abdominal ganglia (Torfs et al., 1999). In the shrimp *Penaeus vannamei*, pevkinin (PevK)-like immunolabeling includes a subset of neurosecretory cells in the brain and thoracic ganglion (Nieto et al., 1998). Supporting a hormonal action for kinin peptides is the finding that, in *Leucophaea*, leucokinin peptides influence the Malpighian tubes and the hindgut but neither structure is innervated by KLI axons (Nässel et al., 1992). Furthermore, kinins are released into the circulation during feeding in the blood-feeding bug, *Rhodnius prolixus* (Te Brugge and Orchard, 2002).

In this report, we identify KLI in the pericardial organs (POs) of the crab *Cancer borealis* and characterize the pevkinin actions in the stomatogastric nervous system (STNS). The crab STNS is composed of four interconnected ganglia plus their connecting and peripheral nerves (Harris-Warrick et al., 1992; Nusbaum and Beenhakker, 2002). The four ganglia include the paired commissural ganglia (CoGs; containing ~550 neurons each) plus the unpaired stomatogastric (STG; 26 neurons) and esophageal (OG; 14 neurons) ganglia (Kilman and Marder, 1996). Most of the STG neurons are components of the gastric mill (chewing) and/or pyloric (filtering of chewed food) motor circuits. These circuits generate multiple versions of the gastric mill and pyloric rhythms due to modulatory inputs they receive from neuronal and hormonal sources (Nusbaum et al., 2001; Marder and Thirumalai, 2002; Marder et al., 2005).

Superfusion of pevkinin to the isolated STG initiated or enhanced the pyloric rhythm. These pevkinin actions included a strong excitation of the lateral pyloric (LP) neuron, whose strengthened inhibitory feedback synapse onto the pyloric pacemaker neurons limited the pevkinin-mediated increase in the pyloric cycle frequency. In contrast, this peptide neither elicited the gastric mill rhythm nor altered its ongoing activity. Because pevkinin selectively excited the pyloric rhythm, we determined whether this action altered the previously documented weakening of the pyloric rhythm during the protractor phase of the gastric mill rhythm. However, there was no evident change in this inter-circuit regulation during pevkinin application.

Some of this work has appeared in abstract form (Hertzberg et al., 2002).

Materials and methods

Animals

Male Jonah crabs (*Cancer borealis* Stimpson) were obtained from a commercial supplier (Commercial Lobster and Seafood, Boston, MA, USA) and from the Marine Biological Laboratory (Woods Hole, MA, USA). Before experimentation, the crabs were housed in commercial tanks containing recirculating, filtered and aerated artificial seawater (10–12°C). Before dissection, the crabs were cold-anesthetized by packing them in ice for at least 30 min. The foregut was then removed and maintained in chilled physiological saline while the STNS was dissected away from the foregut. For tissue collection, the foregut, eyestalks and dorsolateral portions of the pericardial chamber were removed. The STNS, sinus glands (SGs) and POs were subsequently dissected from these structures, respectively, in chilled (approximately 4°C) physiological saline [composition in mmol l^{-1} for physiology experiments: 440 NaCl, 26 $MgCl_2$, 13 $CaCl_2$, 11 KCl, 10 Trizma base, and 5 maleic acid, pH 7.4–7.6; composition in mmol l^{-1} for anatomy experiments: 440 NaCl, 26 $MgCl_2$, 13 $CaCl_2$, 11 KCl, 10 Hepes acid, pH 7.4 (adjusted with NaOH)]. After dissection, the tissue was pinned in a Sylgard 184 (KR Anderson, Santa Clara, CA, USA)-lined Petri dish.

Whole-mount immunocytochemistry

All immunoprocessing was done as whole mounts. Tissue was pinned in a Sylgard-lined Petri dish and fixed in a solution of 4% paraformaldehyde in 0.1 mol l^{-1} sodium phosphate buffer (pH 7.4) for 12–24 h at 4°C. After fixation, tissue was rinsed five times over approximately 5 h, in a solution of sodium phosphate buffer containing 0.3% Triton X-100 (P-Triton). The tissue was then incubated for approximately 72 h in a 1:300 dilution [P-Triton with 10% normal donkey serum (NDS; Jackson ImmunoResearch, West Grove, PA, USA)] of rabbit polyclonal leucokinin I antiserum (Nässel et al., 1992). This antiserum binds with the carboxyl-terminal region of leucokinin I (Nässel et al., 1992). This region of the leucokinin I peptide is similar to the comparable region of the previously identified crustacean kinins, pevkinin (PevK) 1-6 (Nieto et al., 1998; Torfs et al., 1999). The tissue incubation in primary antiserum was followed by another five rinses over approximately 5 h in P-Triton. After this set of rinses, the tissue was incubated for 12–24 h in a 1:300 dilution (as per the primary antiserum) of donkey anti-rabbit IgG conjugated to Alexa Fluor 488 (Molecular Probes, Eugene, OR, USA) or Alexa Fluor 594 (Molecular Probes). After secondary antibody incubation, preparations were rinsed five times over approximately 5 h in sodium phosphate buffer and then mounted between a glass microscope slide and coverslip using Vectashield mounting medium (Vector Laboratories, Inc., Burlingame, CA, USA). Incubations in primary and secondary antisera were done using gentle agitation at 4°C. All rinses were done at room temperature (approximately 20°C) without agitation. Incubation in secondary antibody was conducted in the dark, as was all subsequent processing. Likewise, slides were stored in the dark at 4°C until examination. Specificity controls for the leucokinin I antiserum in *Cancer* tissues are described in Fu et al. (Fu et al., 2005).

Immunolabeled preparations were viewed and data collected using a Bio-Rad Radiance 2000 laser scanning confocal microscope. Descriptions of the hardware and software used for imaging on this system were documented previously (Messinger et al., 2005).

For the production of figures, Bio-Rad.pic files collected using the Radiance 2000 system were converted to .tif files using ImageJ software (freely available at http://rsb.info.nih.gov/ij/). Individual micrographs and composite figures were produced from the tif files using a combination of ImageJ and Photoshop (version 7.0; Adobe Systems Inc., San Jose, CA, USA). The contrast and brightness of final figures were adjusted as needed to optimize the clarity of printed images. Schematic diagrams were produced using Canvas (version 8.0; Deneba Systems Inc., Miami, FL, USA).

Pevkinin peptides

The pevkinins were first isolated and identified in the shrimp *Penaeus vannamei* (Nieto et al., 1998; Torfs et al., 1999). A subset of the pevkinins (PevK-1, PevK-3, PevK-4) have the same carboxyl-terminal amino acid sequence as the insect kinins, including the leucokinins (Torfs et al., 1999). In a

limited, previous study of the actions of the leucokinins on the *C. borealis* STNS, these peptides had a modest excitatory action on the pyloric rhythm (Blitz et al., 1995). To determine whether this modest action resulted from the use of a kinin peptide with the incorrect carboxyl-terminal sequence, we determined whether superfusion of a crustacean kinin peptide with a distinct carboxyl-terminal sequence (PevK-2: Asp-Phe-Ser-Ala-Trp-Ala-NH_2) elicited a stronger response from the *C. borealis* pyloric circuit. In a smaller number of experiments, we also assessed the actions of a second such crustacean kinin (PevK-6: Ala-Phe-Ser-Pro-Trp-Ala-NH_2). PevK-2 was synthesized by the Protein Chemistry Laboratory at the University of Pennsylvania School of Medicine, USA and at the Katholieke Universiteit Leuven, Belgium. PevK-6 was synthesized at the Katholieke Universiteit Leuven, Belgium. Each peptide was stored as a frozen stock solution (10^{-3} mol l^{-1}) that was diluted to its working concentration with *C. borealis* saline immediately before its use. Both peptides were applied to the STNS by superfusion (7–10 ml min^{-1}) to the desheathed STG.

Electrophysiology

Electrophysiological experiments were performed using standard techniques for this system (Beenhakker and Nusbaum, 2004). In brief, the isolated STNS was pinned down in a Sylgard 184-lined Petri dish (Fig. 1). During experiments in which the dorsal posterior esophageal nerve (*dpon*) was stimulated to elicit the gastric mill rhythm, the CoGs remained connected with the STG. In all other experiments, the CoGs were removed to eliminate descending projection neuron influence on the STG circuits. All preparations were superfused continuously with *C. borealis* physiological saline (10–12°C).

Extracellular recordings were made by pressing stainless steel wire electrodes into the Sylgard alongside the nerves and isolating each area with Vaseline. These electrodes were led to a differential AC amplifier (AM Systems, Model 1700, Carlsborg, WA, USA). To facilitate intracellular recordings, desheathed ganglia were viewed with light transmitted through a dark-field condenser (Nikon, Tokyo, Japan). Intracellular recordings of STG somata were made using microelectrodes (15–30 MΩ) filled with 4 mol l^{-1} potassium acetate plus 20 mmol l^{-1} KCl or 0.6 mol l^{-1} K_2SO_4 with 20 mmol l^{-1} KCl. Intracellular recordings and current injections were performed using Axoclamp 2 amplifiers (Axon Instruments, Foster City, CA, USA) in single-electrode discontinuous current-clamp (DCC) mode. Sample rates during DCC were 2–3 kHz. In some preparations, the projection neuron MCN1 was stimulated extracellularly *via* the inferior esophageal nerve (*ion*; 10-30 Hz) (Bartos and Nusbaum, 1997). The *ion* was stimulated using a Grass S88 stimulator and Grass SIU5 stimulus isolation unit (Astro-Med/Grass Instruments, West Warwick, RI, USA).

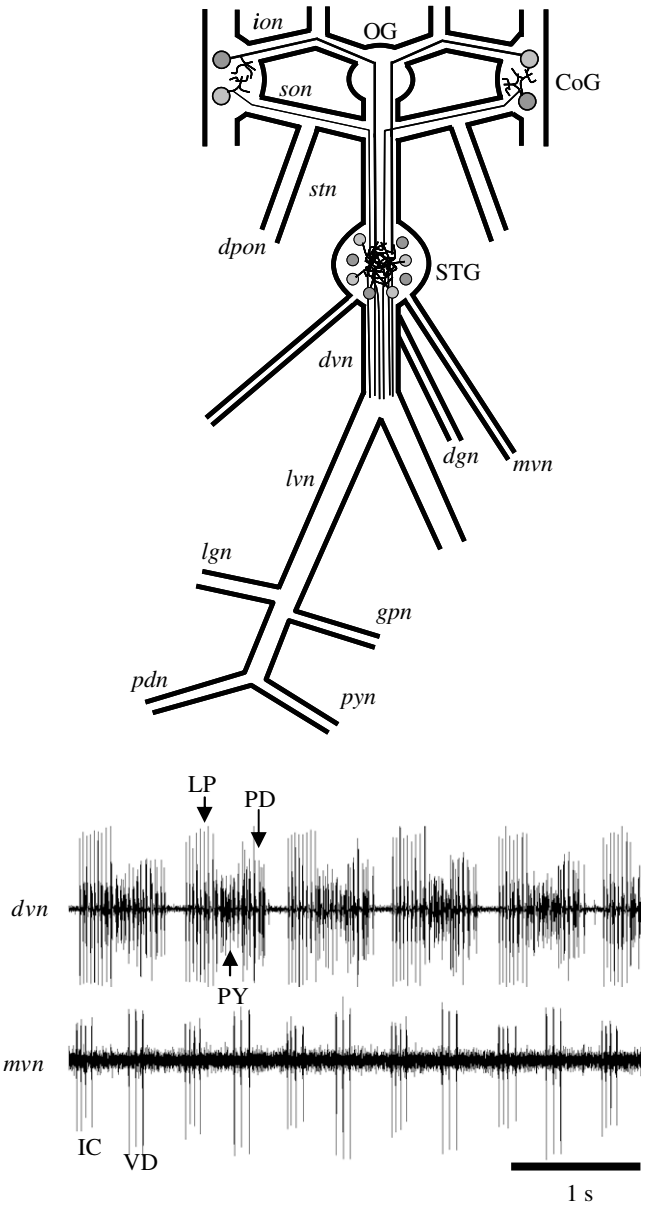

Fig. 1. Schematic of the stomatogastric nervous system of *Cancer borealis* and recordings of the spontaneously active pyloric rhythm. (Top) A schematic of the stomatogastric nervous system, which is composed of the paired commissural ganglia (CoGs) and unpaired esophageal (OG) and stomatogastric (STG) ganglia, plus their connecting nerves and a subset of peripheral nerves. Projection neurons from the CoGs innervate the STG and influence the pyloric and gastric mill rhythms. The axons of a subset of these projection neurons are illustrated projecting through the nerves (*ions*, *sons*, *stn*) that connect these ganglia. The axons projecting through the dorsal ventricular nerve (*dvn*) originate from STG motor neurons and innervate identified pyloric and/or gastric mill muscles. (Bottom) Extracellular recordings of the pyloric motor neurons during a spontaneously active pyloric rhythm in the completely isolated stomatogastric nervous system. Each pyloric motor neuron was identified on the basis of the identity of the recorded nerves, the relative timing of the action potential bursts and the relative amplitude of the recorded action potentials. In *C. borealis*, there are single copies of the LP, IC and VD neurons, two copies of the PD neuron and five copies of the PY neuron (Kilman and Marder, 1996).

Individual STG neurons were identified by their axonal pathways, activity patterns and interactions with other neurons (e.g. Fig. 1) (Beenhakker and Nusbaum, 2004; Blitz et al., 2004). Data were collected directly onto a MT-95000 or Everest chart recorder (Astromed), and were simultaneously digitized (approximately 5 KHz) and collected onto a PC computer using data acquisition/analysis tools (Spike2, Cambridge Electronic Design, Cambridge, UK).

Data analysis

Data analysis was facilitated with a custom-written program for Spike2 that determines the activity levels and phase relationships of neurons (freely available at http://www.neurobiologie.de/). Unless otherwise stated, each datum in a data set was derived by determining the average of 10 consecutive impulse bursts. Briefly, burst duration was defined as the duration between the onset of the first and last action potential in an impulse burst. The firing rate of a neuron was defined as the number of action potentials minus 1, divided by the burst duration. The cycle frequency of the pyloric rhythm was determined by calculating the inverse of the period between the onset of two successive pyloric dilator (PD) neuron bursts. Phase analysis was performed on data collected from extracellular recordings. Phase is defined as the latency to occurrence of an event relative to the start of a cycle, divided by the cycle period. Thus, the latency to onset and offset of activity in each pyloric neuron relative to the onset of a PD neuron burst were measured as a fraction of the total pyloric cycle duration. The gastric mill cycle period corresponded to the duration (sec) between the onset of two successive lateral gastric (LG) neuron bursts. The phase relationships among gastric mill neurons were determined relative to a gastric mill cycle as defined by the onset of one LG neuron burst (beginning of the cycle) and the onset of the subsequent LG neuron burst (end of the cycle).

Figures were made from Spike2 files incorporated into Powerpoint graphics programs (Microsoft, Seattle, WA, USA). Statistical analyses were performed with SigmaStat 3.0 and SigmaPlot 8.0 (SPSS, Chicago, IL, USA). Tests of significance were performed using either Student's *t*-test or repeated measures ANOVA. Data are presented as the mean ± s.d.

Results

Kinin-like immunolabeling in Cancer borealis

A polyclonal antibody directed against leucokinin I did not label any structures of the *C. borealis* STNS (*N*=4) (see also Blitz et al., 1995). Because the STG lies within the ophthalmic artery and is thereby exposed to circulating hormones, we also

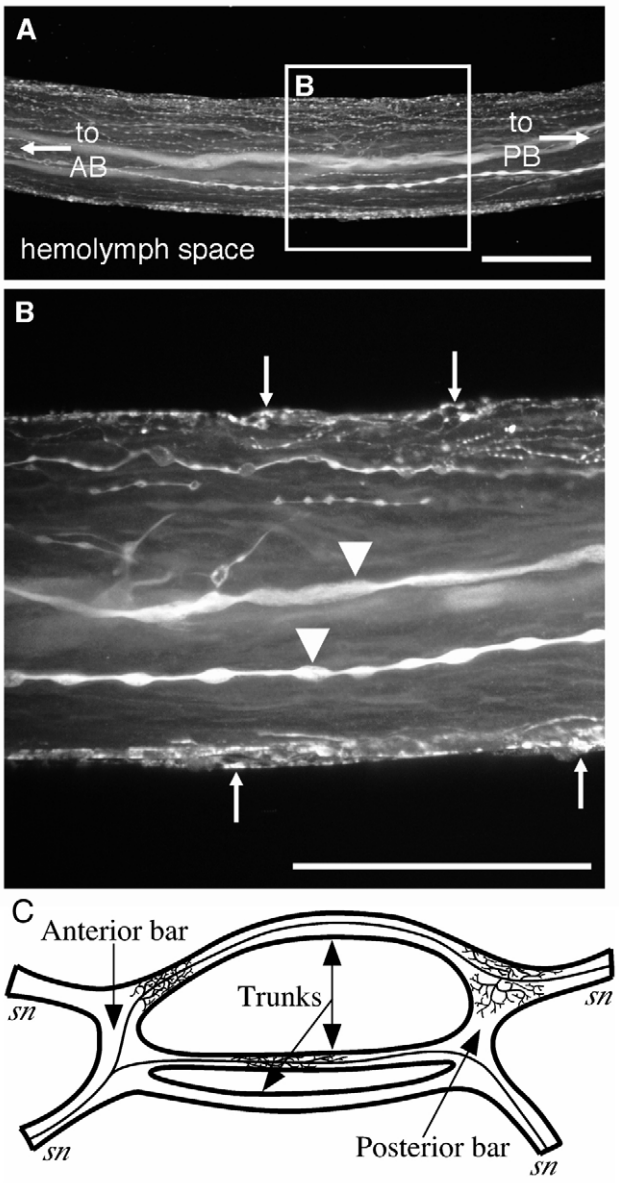

Fig. 2. Kinin-like immunolabeling (KLI) in the pericardial organ (PO) of *Cancer borealis*. (A) KLI in the ventral-most nerve trunk of the PO. This image, a brightest pixel projection of 11 optical sections taken at 1.95 μm intervals, shows that KLI axons, fine neurites and varicosities are present in the PO. Boxed region is shown at a larger scale in B. Scale bar, 100 μm. (B) A higher magnification image of the central core of the nerve trunk. Note that the large diameter immunopositive axons (arrowheads) are present in the center of the trunk, with labeled fine neurites radiating from them toward the perimeter of the nerve where they terminate in a dense network of immunopositive varicosities. Several of these labeled varicosities that appear to be in contact with the hemolymph space are indicated by arrows. This image is a brightest pixel projection of 12 optical sections taken at 0.2 μm intervals. Scale bar, 100 μm. Abbreviations: AB, anterior bar; PB, posterior bar. (C) Schematic representation of KLI in the PO. In brachyuran crabs, including *C. borealis*, each of the bilaterally symmetric POs consists of two or more longitudinal nerve trunks that are connected by vertical nerve bars. The trunks and bars that form each PO are elaborations of the segmental nerves (*sn*) that originate from the thoracic ganglion. In *C. borealis* the distribution of KLI neuropil in each PO, represented in this schematic by the local branching structures, was patchy, variable in location and often restricted to one or more small regions in the nerve trunks that form the PO.

determined whether there was KLI in the major neurohemal structures. There was no KLI in the SG (N=8). However, KLI was present in axons and varicosities in the POs (N=6/8) (Fig. 2). In each of the six preparations that exhibited KLI, the distribution of the labeled varicosities was patchy and was often restricted to one or more small regions in the nerve trunks that form the PO. Moreover, the specific location of KLI was variable between POs.

Pevkinin excites the pyloric rhythm

We assessed the influence of pevkinin on the STG motor circuits primarily by bath application of PevK-2 to the isolated STG. In a few experiments, where noted below, we also assessed the influence of PevK-6. We used the isolated STG in order to have a more consistent control state in which there was no spontaneous input to the STG from modulatory projection neurons. When the CoGs remain connected with the STG during saline superfusion, there is occasionally an ongoing gastric mill rhythm and always a relatively fast pyloric rhythm (cycle frequency: 1–2 Hz), due to input from spontaneously active CoG projection neurons (Fig. 1). Isolating the STG from the CoGs by transection of both superior esophageal nerves (*sons*) and *ions* eliminated the aforementioned inputs, which terminated an active gastric mill rhythm and both slowed and weakened the pyloric rhythm (cycle frequency <1 Hz) (e.g. Fig. 3). In some of these preparations, the pyloric rhythm also terminated.

Application of PevK-2 (10^{-6} mol l^{-1}) to the isolated STG consistently strengthened the pyloric rhythm. This included an increase in both the speed of the ongoing pyloric rhythm and the activity level of several pyloric neurons (Fig. 3). The LP neuron activity was particularly enhanced by PevK-2. By contrast, neither the inferior cardiac (IC) nor ventricular dilator (VD) neurons was activated by PevK-2 (10^{-6} mol l^{-1}; N=30) (e.g. Fig. 3). As a control to verify that the IC and VD neurons were accessible to activation, in most experiments we also stimulated the identified projection neuron MCN1 by extracellular *ion* stimulation (Bartos and Nusbaum, 1997). In all cases, MCN1 excited the pyloric rhythm and activated the IC and VD neurons (N>20). In the isolated STG, the VD neuron is usually silent while IC neuron activity is sometimes present. When the IC neuron was rhythmically active in saline, PevK-2 application did not change that level of activity (saline, 2.3±1.6 spikes/burst; PevK-2, 2.1±1.2 spikes/burst; N=6, P>0.05).

As mentioned above, in some preparations the pyloric rhythm terminated when the CoGs were removed. In every one of the 7 preparations where the pyloric rhythm was not active during saline superfusion, PevK-2 application (10^{-6} mol l^{-1}) initiated this rhythm (Fig. 4). The mean pyloric cycle frequency and number of LP spikes per burst in these preparations (cycle frequency: 0.53±0.15 Hz, no. LP spikes/burst: 15.1±7.3; N=7) were comparable to those occurring during PevK-2 application in preparations with slow but persisting pyloric rhythms (see below).

In preparations with ongoing pyloric rhythms during saline superfusion, the fastest pyloric cycle frequency occurring during PevK-2 application (10^{-6} mol l^{-1}) was 1.03 Hz. However, the mean cycle frequency that occurred during these PevK-2 applications was considerably slower (saline, 0.59±0.2 Hz; PevK-2, 0.71±0.14 Hz; N=30, P<0.0001). As shown by the scatter plot in Fig. 5, within the range of control values examined, PevK-2 (10^{-6} mol l^{-1}) usually increased the pyloric rhythm speed. It is noteworthy,

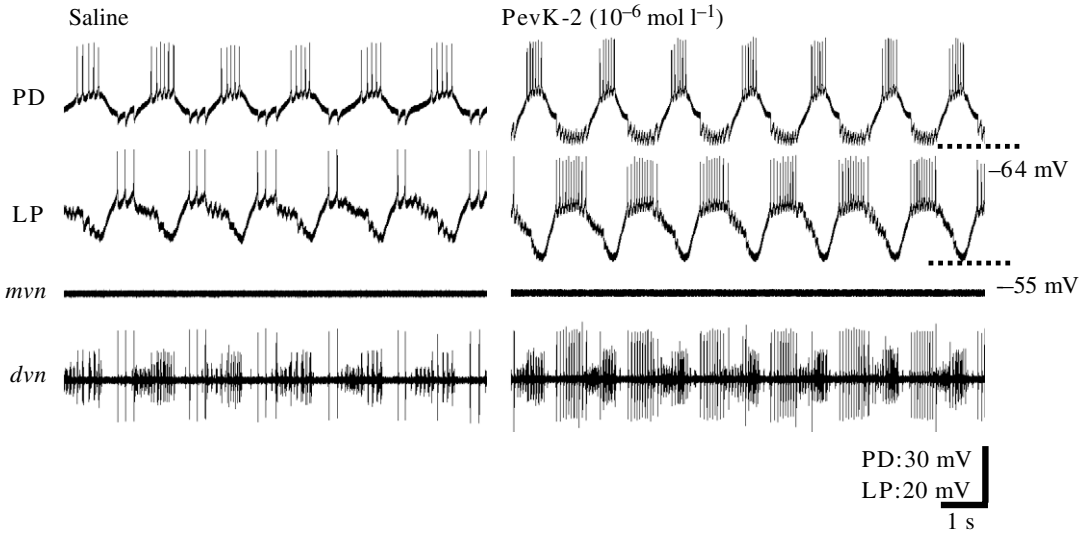

Fig. 3. Pevkinin-2 excites the pyloric rhythm. (Left) During saline superfusion in a preparation where the STG was isolated from the CoGs, there was an ongoing pyloric rhythm. Note that, without the influence of spontaneously active CoG projection neurons, the pyloric rhythm was relatively slow and weak (see Fig. 1). (Right) During superfusion of pevkinin-2 (PevK-2), there was an increased pyloric rhythm speed as well as increased activity in the PD and LP neurons. Note also the increased number and amplitude of the LP-mediated IPSPs in the PD neuron during PevK-2 superfusion. The IC and VD neurons (*mvn*) were not activated by PevK-2 application.

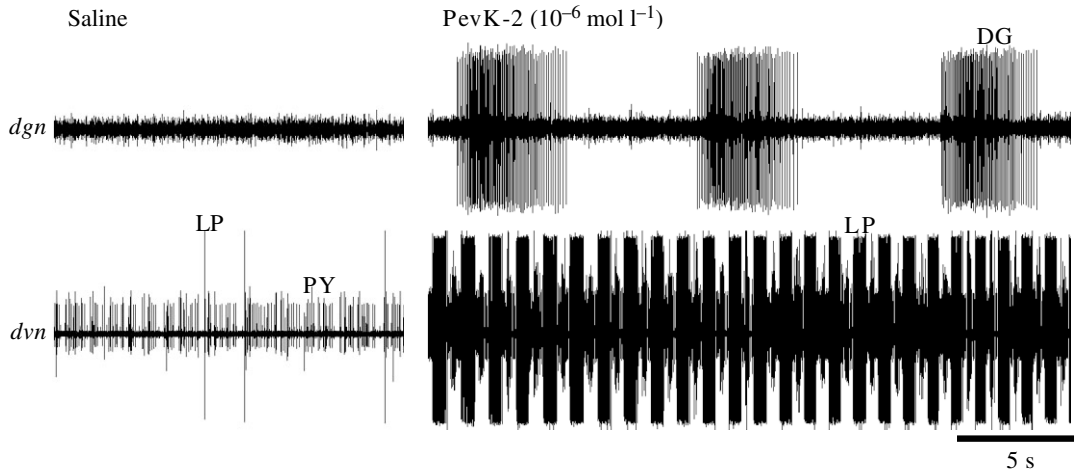

Fig. 4. Pevkinin-2 initiates the pyloric rhythm and elicits slow, rhythmic bursting in a gastric mill motor neuron. (Left) During saline superfusion in the isolated STG, there was no pyloric rhythm (*dvn*) and the dorsal gastric (DG) neuron was inactive (*dgn*). Note that the there was ongoing tonic activity in the PY neurons and occasional action potentials in the LP neuron, while the PD neurons were silent. (Right) Superfusion of PevK-2 initiated the pyloric rhythm and elicited rhythmic bursting in the DG neuron. There was no temporal relationship evident between the bursting patterns of the pyloric rhythm and the DG neuron.

however, that not all of the preparations having a relatively fast pyloric rhythm (>0.5 Hz) during saline superfusion exhibited an increased cycle frequency in the presence of PevK-2 (Fig. 5). This inconsistent result of PevK-2 at faster control levels might have been a consequence of the PevK-2 excitation of the LP neuron (see below). We did not assess the influence of PevK-2 on pyloric rhythms faster than 1 Hz because this situation rarely occurred in the isolated STG during saline superfusion.

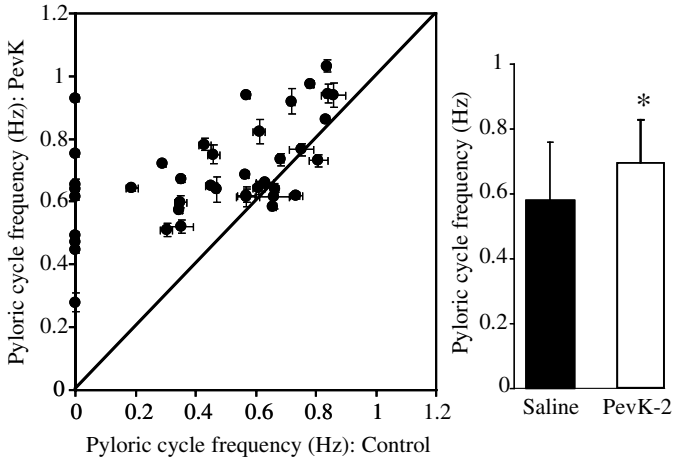

Fig. 5. Pevkinin-2 increases the speed of the pyloric rhythm. (Left) Scatter plot of the pyloric cycle frequency during superfusion of PevK-2 (10^{-6} mol l^{-1}) as a function of the pyloric cycle frequency during saline superfusion. Each data point represents the mean (±s.d.) cycle frequency from a single experiment during PevK-2 superfusion and its pre-application control (*N*=39). Data points located along the diagonal, unity line indicate experiments in which PevK-2 application did not change the ongoing cycle frequency. (Right) PevK-2 (10^{-6} mol l^{-1}) application increased the mean pyloric cycle frequency across preparations (*N*=39; **P*<0.0001).

In contrast to the ability of PevK-2 to consistently increase the speed of the pyloric rhythm, superfusion of PevK-6 (10^{-6} mol l^{-1}) was not as effective at changing the speed of this rhythm (saline, 0.47±0.33 Hz; PevK-6, 0.80±0.18 Hz; *N*=6, *P*>0.05). This was the case even when they were applied to the same STG (*N*=6). Despite this discrepancy, PevK-6 application was as effective as PevK-2 in enhancing LP neuron activity (saline, 3.6±2.1 spikes/burst; PevK-2, 11.6±3.6 spikes/burst, *N*=40; PevK-6, 14.4±3.2 spikes/burst; *N*=6; PevK-2 and PevK-6 relative to saline: *P*<0.001; PevK-2 *versus* PevK-6: *P*>0.05) (Fig. 6). Unlike the response of the pyloric cycle frequency to PevK-2 application (Fig. 5), the increased number of spikes per burst in the LP neuron in response to PevK-2 occurred in every preparation, across the entire range of control values (Fig. 6). The PevK-mediated excitation of the LP neuron also included a significant increase in its intra-burst firing frequency. This LP neuron parameter nearly doubled during PevK-2 superfusion (saline, 11.3±4.6 Hz; PevK-2, 21.6±4.9 Hz, *N*=35, *P*<0.001).

The LP neuron directly inhibits the PD neuron and, through electrical coupling between the PD and AB neurons, it also inhibits the AB neuron (Eisen and Marder, 1982). Thus, during PevK superfusion, strengthened LP neuron activity resulted in an increased amplitude and frequency of LP-mediated IPSPs in the electrically coupled pyloric pacemaker neurons (e.g. PD neuron in Fig. 3; see also below). Additionally, the LP neuron burst duration was increased in the presence of PevK-2 (saline, 0.26±0.1 s.; PevK-2, 0.47±0.15 s., *N*=30; *P*<0.0001). This increased burst duration resulted in an increased duration of LP-mediated inhibition in the pyloric pacemaker neurons (e.g. Fig. 3). In contrast, PevK-2 superfusion did not alter the PD neuron burst duration (saline, 0.29±0.15 s.; PevK-2, 0.24±0.08 s., *N*=7; *P*>0.05). However, PevK-2 (10^{-6} mol l^{-1})

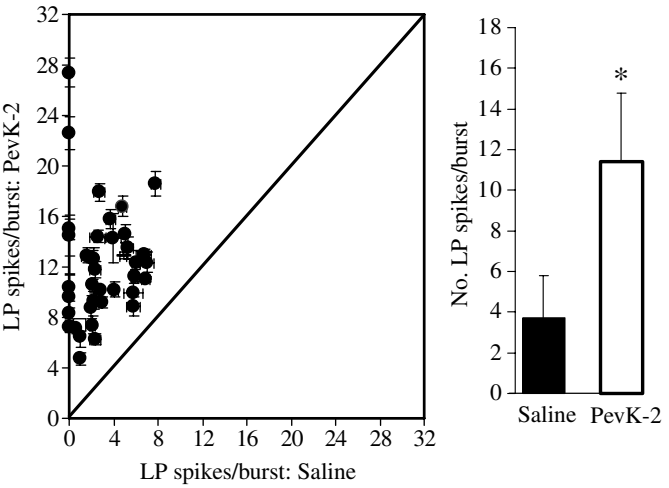

Fig. 6. Pevkinin-2 increases the pyloric rhythm-timed activity level of the LP neuron. (Left) Scatter plot of the number of LP neuron spikes/burst in PevK-2 (10^{-6} mol l^{-1}; N=40) as a function of LP neuron activity during saline superfusion. Each data point represents the mean (±s.d.) number of LP spikes/burst from a single experiment during PevK-2 superfusion and its pre-application control. The diagonal, unity line indicates the points at which PevK-2 application and saline superfusion resulted in the same level of LP neuron activity. (Right) PevK-2 (N=32) increased the mean number of LP spikes/burst, relative to saline controls, during the ongoing pyloric rhythm (*P<0.0001).

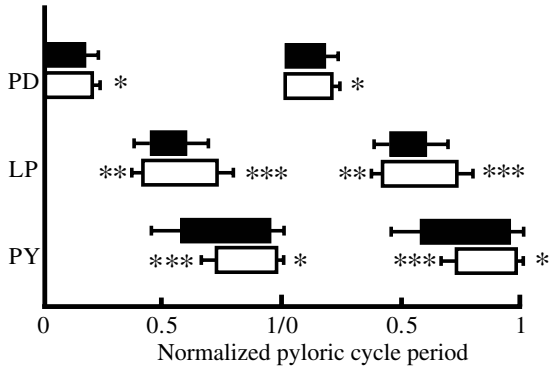

Fig. 7. Pevkinin-2 alters the phase relationships among the pyloric neurons. The phase relationships of the pyloric neurons PD, LP and PY are plotted as a function of the normalized pyloric cycle period during saline (filled boxes) and PevK-2 (open boxes) superfusion. A single pyloric cycle extends from the onset of the PD neuron burst to the start of the next PD neuron burst. All five analyzed parameters (mean phase offset of the PD neuron burst, mean phase onset and offset of the LP and PY neuron bursts) were changed during PevK-2 (10^{-6} mol l^{-1}) superfusion (N=22; *P<0.05, **P<0.01, ***P<0.001).

superfusion did increase both the number of PD neuron spikes/burst (saline, 3.6±1.6 spikes; PevK-2, 5.0±1.7 spikes, N=7, P<0.05) and its intra-burst firing frequency (saline, 8.4±3.3 Hz; PevK-2, 17.0±7.3 Hz; N=7, P<0.05).

Application of PevK-2 to the isolated STG did not change the relative progression of rhythmic, repeating activity in the pyloric neurons PD, LP and PY. However, it did change the fraction of a normalized pyloric cycle during which each of these neurons was active ('duty cycle'). Specifically, there was an increase in the PD and LP neuron duty cycles and a decreased duty cycle in the PY neurons (Fig. 7). The increased PD neuron duty cycle resulted in an increase in the cycle phase (latency from cycle onset to measured parameter divided by the cycle period) at which its burst terminated (Fig. 7). PD neuron burst onset defines the start and end of each pyloric cycle, precluding there being any change in the cycle phase at which its burst begins. The increased LP neuron duty cycle resulted from its mean burst onset being phase advanced and its burst offset being phase delayed relative to saline controls (Fig. 7). The decreased PY neuron duty cycle resulted largely from the phase delay in its burst onset relative to saline controls (Fig. 7). There was also a smaller but significant phase delay in its mean burst offset.

We also assessed the influence of PevK-2 on the pyloric rhythm when applied at different concentrations. Surprisingly, we found that the PevK-2 actions on the pyloric rhythm cycle frequency and LP neuron activity had different thresholds (Fig. 8). Specifically, the threshold for PevK-2 excitation of the LP neuron was 10^{-7} mol l^{-1}, whereas its ability to increase the pyloric cycle frequency had a threshold of 10^{-6} mol l^{-1} (Fig. 8A,B). However, the PevK-2 excitation of the LP neuron was stronger at 10^{-6} mol l^{-1} than at the lower concentration (Fig. 8B).

LP neuron regulation of the pyloric rhythm during pevkinin application

As indicated above, when the control pyloric rhythms were faster than 0.5 Hz, PevK-2 application did not increase the speed of the rhythm in all preparations (Fig. 5). We therefore assessed whether this variability might have resulted from the strengthened LP neuron inhibition of the pyloric pacemaker group limiting the increase in cycle speed in these preparations. The pyloric rhythmicity originates largely from the intrinsic properties of the anterior burster (AB) neuron, which is a conditionally active endogenous oscillator (Miller and Selverston, 1982). There are two sources of pyloric circuit regulation of the intrinsic rhythmicity of the AB neuron, including its electrical coupling to the PD neurons and the feedback inhibition that it receives through that electrical coupling, as a result of LP neuron inhibition of the PD neuron (Hooper and Marder, 1987; Ayali and Harris-Warrick, 1999). To determine whether the strong PevK-2 excitation of the LP neuron was limiting the ability of this peptide to increase the speed of the rhythm, we compared the pyloric rhythm cycle frequency during PevK-2 (10^{-6} mol l^{-1}) superfusion with the LP neuron active and inactive. LP neuron activity was readily suppressed by hyperpolarizing current injection. As shown in Fig. 9A, suppressing LP neuron activity did not alter the speed of the pyloric rhythm during saline superfusion. By contrast, performing the same manipulation during PevK-2 superfusion did indeed increase the ongoing pyloric cycle frequency (Fig. 9B). Note that, whenever the LP neuron activity was suppressed, the LP-mediated IPSPs in the PD neuron were

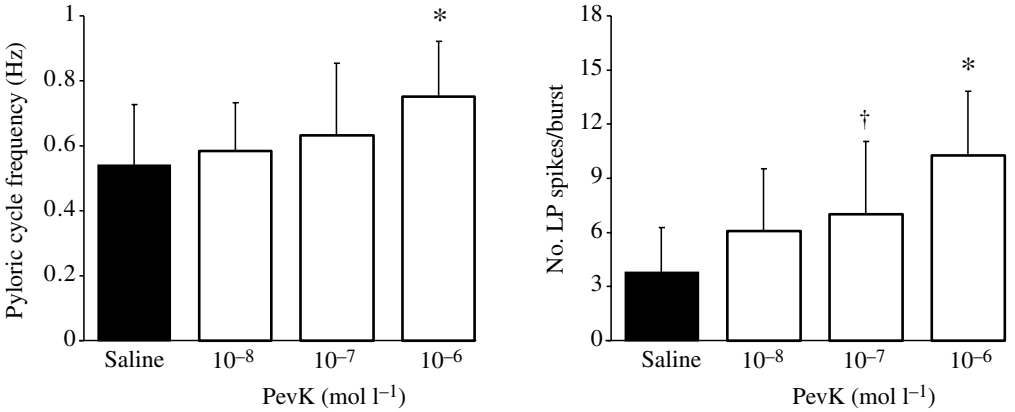

Fig. 8. The actions of pevkinin-2 on the pyloric rhythm are dose dependent. (Left) PevK-2 application had dose-dependent actions on the pyloric cycle frequency. As shown in Fig. 5, PevK-2 (10^{-6} mol l^{-1}) increased the pyloric cycle frequency relative to saline controls. However, the pyloric cycle frequency was unchanged during application of lower peptide concentrations. (Right) PevK-2 superfusion increased the number of LP neuron spikes/burst in a dose-dependent manner. The threshold concentration for PevK-2 enhancement of LP neuron activity (10^{-7} mol l^{-1}), relative to levels during saline superfusion, was lower than for pyloric cycle frequency (10^{-6} mol l^{-1}). The mean number of LP neuron spikes/burst was also larger when PevK-2 was applied at 10^{-6} mol l^{-1} than at 10^{-7} mol l^{-1} (N=6 or 7 for each concentration; *P<0.005, †P<0.05).

eliminated and the trough of the PD neuron membrane potential oscillations were depolarized. This effect on pyloric cycle frequency was consistent across preparations (saline with LP active, 0.49±0.15 Hz; saline with LP silent, 0.55±0.13 Hz, N=9, P>0.05; PevK-2 with LP active, 0.68±0.13 Hz; PevK-2 with LP silent, 0.96±0.12 Hz, N=9, P<0.001) (Fig. 10).

Pevkinin minimally alters the VCN-elicited gastric mill rhythm

Despite consistently altering the pyloric rhythm, PevK-2 (10^{-6} mol l^{-1}) superfusion never activated the gastric mill rhythm in the isolated STG (N=40). However, in these preparations, bath application of this peptide did consistently and reversibly elicit rhythmic bursting in one gastric mill retractor motor neuron, the dorsal gastric (DG) neuron (Fig. 4). In general, the DG neuron was silent during saline superfusion (N=22/25 preparations) (e.g. Fig. 4). In three of these preparations, this neuron instead exhibited spontaneous rhythmic bursting, with an erratic cycle period, during saline superfusion. In 23 of these same 25 preparations, superfusion of PevK-2 or PevK-6 (10^{-6} mol l^{-1}) elicited regular DG neuron

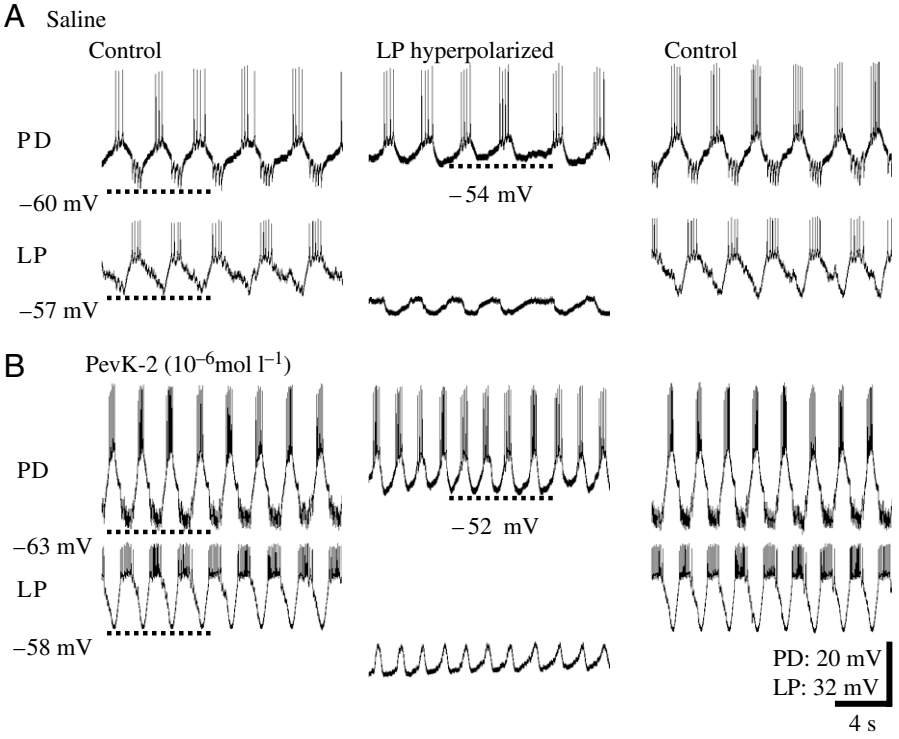

Fig. 9. The LP neuron regulates the speed of the pevkinin-modulated pyloric rhythm. (A) Suppressing LP neuron activity during an ongoing pyloric rhythm in saline did not alter the pyloric cycle frequency. Note that there were five pyloric cycles (six PD neuron bursts) in the same duration regardless of whether the LP neuron was active (pre- and post-LP hyperpolarization) or was silenced (middle) by constant amplitude hyperpolarizing current injection. The pyloric rhythm was unchanged despite the fact that, when LP was silenced, the LP-mediated IPSPs were eliminated in the PD neuron and the trough of the PD neuron slow wave oscillation was depolarized. (B) Suppressing LP neuron activity during an ongoing pyloric rhythm in the presence of PevK-2 increased the pyloric cycle frequency. During the same duration, there were seven pyloric cycles when the LP neuron was active both pre- and post-LP hyperpolarization whereas there were ten pyloric cycles when LP activity was suppressed by hyperpolarizing current injection. Traces in A and B are from the same experiment.

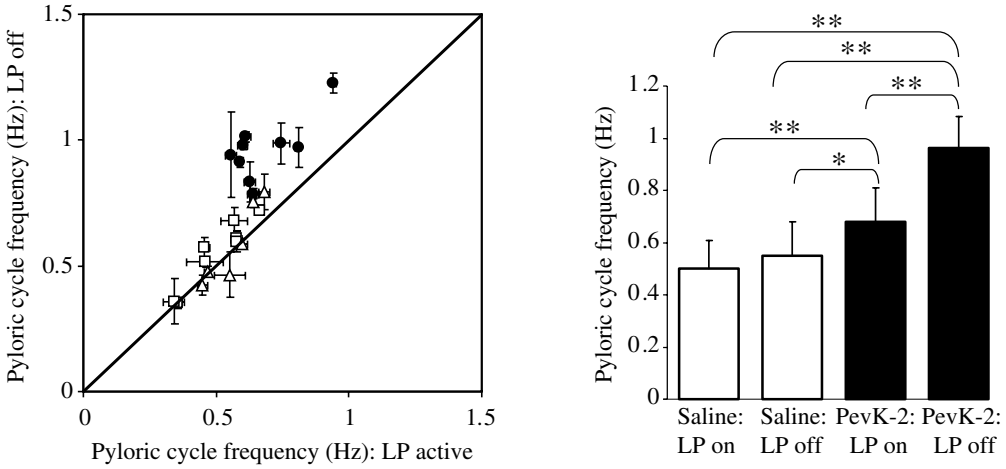

Fig. 10. The LP neuron regulates the speed of the pevkinin-modulated pyloric rhythm. (Left) Scatter plot comparing the pyloric cycle frequency when the LP neuron was active and silent, during both saline superfusion (pre-PevK-2, open squares; post-PevK-2, open triangles) and PevK-2 (10^{-6} mol l^{-1}) application (filled circles). The LP neuron was silenced *via* hyperpolarizing current injection (see Fig. 9). During saline superfusion, suppressing LP neuron activity generally did not alter the mean pyloric cycle frequency. Note that these data points lie along the diagonal, unity line. By contrast, during PevK-2 superfusion, suppressing LP neuron activity consistently increased the pyloric cycle frequency relative to times during the same preparation when the LP neuron was active. (Right) Across preparations, the mean pyloric cycle frequency during saline superfusion was unchanged by suppressing LP neuron activity. However, during PevK-2 application, suppressing LP neuron activity did increase the pyloric cycle frequency. Both examined conditions during PevK-2 application resulted in faster pyloric rhythms than either condition examined during saline superfusion (N=9; *P<0.05, **P<0.001).

bursting that persisted for the duration of peptide application (DG burst duration: 11.06±4.0 s; DG intraburst firing frequency: 9.27±1.3 Hz; DG cycle period: 39.5±12.5 s; N=23). This rhythmic DG neuron activity was independent of the activity pattern of all other STG neurons (e.g. Fig. 4). The activity of none of the other gastric mill neurons was altered by PevK superfusion (data not shown).

As is the case for the pyloric rhythm, there are several distinct versions of the gastric mill rhythm (Blitz and Nusbaum, 1997; Beenhakker and Nusbaum, 2004; Blitz et al., 2004; Wood et al., 2004). Unlike the pyloric rhythm, the gastric mill rhythm is usually not spontaneously active in the isolated STNS. However, it can be readily activated by stimulation of the appropriate pathway(s). To determine whether pevkinin also influenced the gastric mill rhythm, we focused our experiments on gastric mill rhythms activated by extracellular stimulation of the mechanosensory ventral cardiac neurons (VCNs) (Beenhakker et al., 2004). We selected this gastric mill rhythm because a relatively brief VCN stimulation (1–2 min) triggers a long-lasting gastric mill rhythm that is stable for tens of minutes. This gastric mill rhythm results from the VCNs triggering a persisting activation of two identified projection neurons, including modulatory commissural neuron 1 (MCN1) and commissural projection neuron 2 (CPN2), in the commissural ganglia (Beenhakker and Nusbaum, 2004). These two projection neurons in turn drive the gastric mill rhythm. The VCN-elicited gastric mill rhythm is characterized by rhythmic bursting of the LG, GM, IC and MG protractor phase neurons alternating with the retractor phase neurons Int1, DG, VD and AM (Beenhakker et al., 2004; Beenhakker and Nusbaum, 2004) (see Fig. 11).

The VCN-elicited gastric mill rhythm was only minimally altered by the presence of PevK-2 (10^{-6} mol l^{-1}; N=7; Figs 11, 12). For example, peptide superfusion did not alter either the speed of the gastric mill rhythm or the activity of the gastric mill neurons (Fig. 12). This included no change in the activity

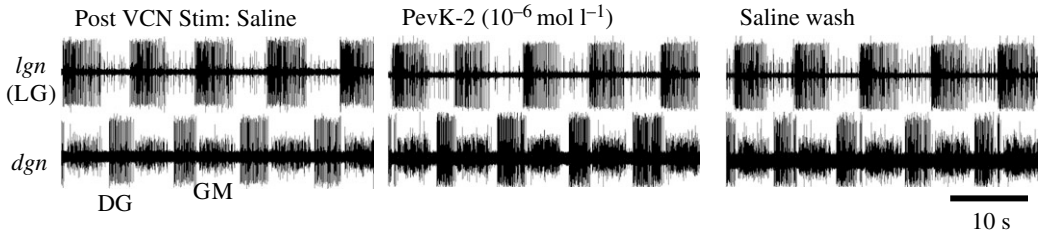

Fig. 11. The VCN-elicited gastric mill rhythm was not altered by pevkinin-2 application. There was no evident alteration in the VCN-elicited gastric mill rhythm during superfusion of PevK-2 (10^{-6} mol l^{-1}). These three gastric mill rhythms were elicited, in the same preparation, by three separate VCN stimulations, performed in the order shown.

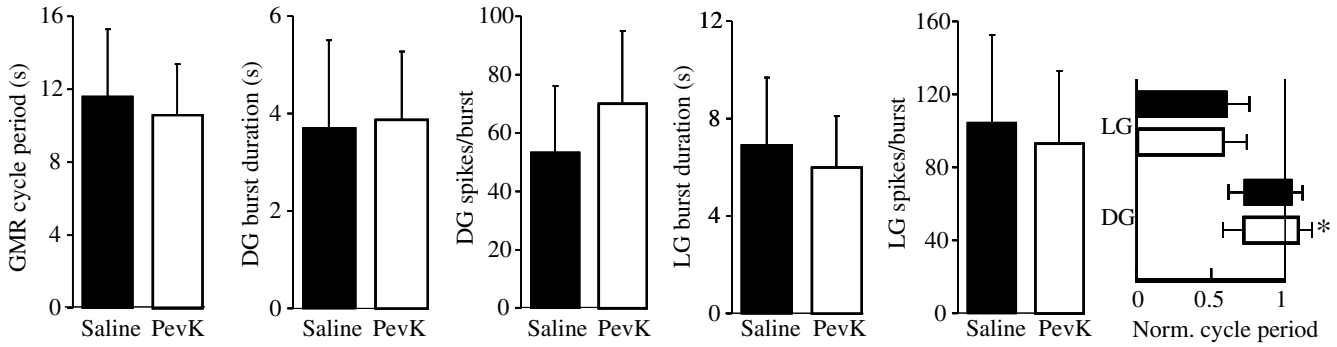

Fig. 12. The VCN-elicited gastric mill rhythm is largely unchanged by the presence of pevkinin-2. Superfusion of PevK-2 (10^{-6} mol l^{-1}) did not alter most of the analyzed parameters of the VCN-elicited gastric mill rhythm. The only change occurred in the DG neuron mean burst offset phase, which was delayed by peptide application (N=7; P<0.05).

of the DG retractor neuron, which as indicated above was consistently activated to burst rhythmically by PevK application in the absence of the gastric mill rhythm. For example, neither the DG neuron burst duration nor intraburst firing frequency was altered by PevK-2 (10^{-6} mol l^{-1}) superfusion during the VCN-elicited gastric mill rhythm (DG burst duration: saline, 2.8±0.8 s; PevK-2, 3.6±1.6 s; DG intraburst firing frequency: saline, 16.22±3.9 Hz; PevK-2, 18.6±3.8 Hz; N=7, P>0.05) (Fig. 12). Similarly, PevK superfusion caused no change in the LG protractor neuron burst duration or its intraburst firing frequency (LG burst duration: saline, 6.88±3.3 s; PevK-2, 6.21±2.5 s; LG intraburst firing frequency: saline, 15.78±4.6 Hz; PevK-2, 15.98±4.3 Hz; N=7, P>0.05) (Fig. 12). There was, however, a small but significant phase delay in the termination of the DG neuron burst when PevK-2 was superfused during the VCN-elicited gastric mill rhythm (Fig. 12).

Previous studies showed that the gastric mill rhythm elicited by selective stimulation of MCN1 causes a slowing and weakening of the pyloric rhythm during the gastric mill protractor phase (Bartos and Nusbaum, 1997). This action results from the rhythmic presynaptic inhibition of the STG terminals of MCN1 by the LG protractor neuron, which reduces MCN1 excitation of the pyloric rhythm. After finding that pevkinin excited the pyloric rhythm but did not alter the VCN-elicited gastric mill rhythm, we tested the hypothesis that superfusion of this peptide reduced or eliminated the gastric mill protractor-timed slowing and weakening of the pyloric rhythm. We found that PevK-2 superfusion (10^{-6} mol l^{-1}) did not rescue the pyloric rhythm from the inhibitory influence of the gastric mill rhythm. For example, as shown previously for the MCN1-elicited gastric mill rhythm, the pyloric cycle frequency was consistently slowed during the gastric mill protractor phase when the preparation was superfused with saline (pyloric cycle frequency: retraction phase, 1.26±0.05 Hz; protraction phase, 1.14±0.06 Hz; N=7, P<0.0001). In the same preparations, there was a similar slowing during PevK-2 superfusion (retraction phase, 1.25±0.08 Hz; protraction phase, 1.14±0.08 Hz; N=7, P<0.0001).

Discussion

Previous studies showed that kinin peptides have actions in the periphery, at the level of neuromuscular systems and effector organs (Coast, 1998; Hayes et al., 1989; Te Brugge and Orchard, 2002; Te Brugge et al., 2002; Terhzaz et al., 1999; Torfs et al., 1999). In this paper, we show that pevkinin also modulates motor circuit activity within the crustacean nervous system. Specifically, PevK application to the isolated crab STG routinely excited the pyloric motor rhythm. This PevK action was relatively specific insofar as it had little influence on the gastric mill rhythm, which is also generated in the STG.

Kinins in C. borealis

We found KLI in the pericardial organs, a major neuroendocrine structure in the crab, but not within the STNS. A previous study of kinins in *C. borealis*, using the same anti-leucokinin antiserum used in the present study, had revealed no KLI in the POs (Blitz et al., 1995). This discrepancy might have resulted from alterations in the immunoprocessing methodology. For example, in the earlier work, incubations with antiserum were maintained on a refrigerator shelf instead of undergoing continuous agitation. Alternatively, the KLI in the POs might have been overlooked in the original study because, although found consistently across preparations, the immunolabeling was patchy and restricted to small areas of the POs. Mass spectrometric analysis also supports the presence of PevK-2 in the POs, although the amino acid sequence for the peptide represented by PevK-2-like peak has yet to be definitively identified in this structure (Huybrechts et al., 2003).

Given that kinins are likely to reach the STG *via* hormonal release, it was surprising that the actions of PevK superfusion did not have a lower threshold (Jorge-Rivera and Marder, 1996; Nässel, 2002). For example, previously studied neuroactive peptides native to *C. borealis*, including those that are localized to the POs but not the STNS, were found to have thresholds for excitation of the pyloric rhythm that were lower than those for PevK-2 by several orders of magnitude (Skiebe, 2001). This discrepancy in threshold of action suggests that PevK-2 might not be the kinin native to *C. borealis*. It may well be that the amino acid sequence of the *C. borealis* kinin (cabkinin) differs

slightly from that of the studied pevkinins and that this difference influences the effectiveness of receptor binding. Previous studies of the pyloric rhythm response to several peptide family members, in each case including the peptide(s) native to *C. borealis*, have shown qualitatively consistent effects on the pyloric rhythm but quantitative shifts in the dose–response relationship (Nusbaum and Marder, 1988; Weimann et al., 1993; Christie et al., 1997). Alternatively, cabkinin might be identical to PevK-2 and the unusually high threshold concentration for exciting the pyloric rhythm might result from this peptide being effectively degraded by extracellular peptidase activity within the STG (Coleman et al., 1994; Wood et al., 2000; Wood and Nusbaum, 2002).

Leucokinin, an insect kinin family member, was shown previously to increase both the pyloric cycle frequency and the number of LP spikes per burst, and to elicit rhythmic bursting in the DG neuron (Blitz et al., 1995). Although leucokinin shares these actions with PevK-2, it differs from PevK-2 in that it neither increased the PD neuron duty cycle nor did it phase advance LP neuron burst onset. A more extensive comparison between the actions of the current and previous results with these kinins is not possible, however, because the previous study had a more limited scope (Blitz et al., 1995).

Pevkinin actions on the pyloric circuit

Pevkinin application to the isolated STG consistently excited the pyloric rhythm, either activating the rhythm or enhancing slow rhythms (<0.5 Hz). However, whereas all slow pyloric rhythms exhibited an increased cycle frequency, only a subset of the faster rhythms were sped up during PevK-2 application. By contrast, all preparations exhibited a considerable increase in the level of LP neuron activity during PevK-2 application. The LP neuron is well-positioned to regulate the pyloric cycle frequency because it makes the only inhibitory feedback synapse onto the pyloric pacemaker neurons (Eisen and Marder, 1982). Our results support the hypothesis that the strengthened LP neuron activity is at least partly responsible for the speed of some of the faster control pyloric rhythms being unaffected by PevK-2 application. Similarly, the lower threshold for PevK-2 excitation of the LP neuron relative to the PevK-2 enhancement of the pyloric cycle frequency might be a secondary consequence of the strengthened LP neuron inhibition of the pyloric pacemaker neurons. Although this feedback inhibition is effective during PevK-2 application, the effectiveness of this synapse is state-dependent. For example, despite the ability of other applied modulators to increase LP neuron activity, suppressing this LP neuron activity often has no impact on the speed of the pyloric rhythm (Hooper and Marder, 1987; Ayali and Harris-Warrick, 1999; Thirumalai et al., 2006). This was also the case in our control experiments. The mechanism underlying the enhanced ability of the LP neuron to regulate the pyloric rhythm speed during PevK-2 superfusion, however, awaits further study.

Pevkinin actions on the gastric mill circuit

As shown previously for leucokinin (Blitz et al., 1995), the only gastric mill circuit neuron affected by PevK-2 is the DG neuron. We did not determine whether this PevK action was direct, but the resulting rhythmic bursting in the DG neuron appeared to result from the activation of intrinsic oscillatory properties in this neuron. This conclusion was drawn on the basis of the DG neuron bursting pattern being independent from every other STG neuron. However, we did not eliminate the possibility that PevK application was indirectly influencing the DG neuron by eliciting transmitter release from the STG terminals of one or more projection neurons. These terminals remain functional in the acutely isolated STG, despite the elimination of their somata and arborizations in the CoGs (Nusbaum et al., 1992). In *C. borealis*, comparable independent rhythmic bursting in the DG neuron is also elicited by application of other neuromodulators and by selective stimulation of either an identified proprioceptor neuron or a CoG projection neuron (Katz and Harris-Warrick, 1989; Kiehn and Harris-Warrick, 1992; Coleman and Nusbaum, 1994; Blitz et al., 1995).

Despite the ability of PevK-2 to elicit rhythmic bursting in the DG neuron, it neither elicited nor altered the gastric mill rhythm. It might seem surprising that PevK-2 application did not at least indirectly influence other gastric mill neurons *via* its excitation of the DG neuron. However, this neuron has only inhibitory synaptic actions within the STG and its synaptic targets are not activated upon rebound from this inhibition (Norris et al., 1994; Beenhakker et al., 2005; Stein et al., 2005).

Neuromodulators can also potentially influence inter-circuit interactions. In the *C. borealis* STG, the pyloric and gastric mill circuits influence each other. For example, the pyloric rhythm is slowed and weakened during the protraction phase of the gastric mill rhythm. This effect results from the presynaptic inhibition of the STG terminals of the projection neuron MCN1 by the gastric mill protractor neuron LG, thereby reducing MCN1 excitation of the pyloric rhythm (Bartos and Nusbaum, 1997). This raised the possibility that, by its selective excitation of the pyloric rhythm, PevK-2 would interfere with the gastric mill weakening of the pyloric rhythm by substituting its own excitation of the pyloric rhythm for that contributed by MCN1. However, PevK-2 did not alter the gastric mill regulation of the pyloric rhythm. Although we did not explicitly determine why this was so, it may result from the fact that the pyloric rhythm cycle frequency during the gastric mill protractor phase is comparable to that during PevK-2 superfusion (Bartos and Nusbaum, 1997).

Using the well-characterized circuits in the STG, we have shown that kinin peptides can act within the arthropod CNS to change the output of a rhythmically active motor circuit. Given the previously documented peripheral actions of kinin peptides in other arthropods (Coast, 1998; Hayes et al., 1989; Te Brugge and Orchard, 2002; Te Brugge et al., 2002; Terhzaz et al., 1999; Torfs et al., 1999) and its neurohemal organ localization in *C. borealis*, it may well be that the PevKs further modify the pyloric motor system *via* peripheral actions. The *C. borealis* neuromuscular system is known to be extensively modulated, both pre- and post-synaptically (Jorge-Rivera and Marder, 1996;

Jorge-Rivera et al., 1998; Birmingham et al., 2003; Messinger et al., 2005). Similarly, despite having no central actions on the gastric mill circuit, the PevKs may well also alter the strength and/or pattern of gastric mill muscle contractions. Given the presence of many different neuroactive substances in the POs and in the terminals of projection and sensory neurons that innervate the STG neuropil (Nusbaum et al., 2001; Skiebe, 2001; Marder et al., 2005; Billimoria et al., 2005), it will be informative to determine which of these substances are normally co-released with the native PevK-like peptide in *C. borealis* as well as to determine the consequences of that co-release.

List of abbreviations

AB	anterior burster
AM	anterior median
Cabkinin	*Cancer borealis* kinin
CNS	central nervous system
CoG	commissural ganglion
CPN2	commissural projection neuron 2
DCC	discontinuous current clamp
DG	dorsal gastric
dgn	dorsal gastric nerve
dpon	dorsal posterior esophageal nerve
GM	gastric mill
gpn	gastropyloric nerve
IC	inferior cardiac
ion	inferior esophageal nerve
IPSP	inhibitory postsynaptic potential
KLI	kinin-like immunolabeling
LG	lateral gastric
lgn	lateral gastric nerve
LK	leucokinin
LP	lateral pyloric
lvn	lateral ventricular nerve
MCN1	modulatory commissural neuron 1
MG	medial gastric
mvn	medial ventricular nerve
OG	esophageal ganglion
PD	pyloric dilator
pdn	pyloric dilator nerve
PevK	pevkinin
PO	pericardial organ
PY	pyloric
pyn	pyloric nerve
SG	sinus gland
sn	segmental nerve
son	superior esophageal nerve
STG	stomatogastric ganglion
stn	stomatogastric nerve
STNS	stomatogastric nervous system
VCN	ventral cardiac neuron
VD	ventricular dilator

This work was supported by National Institute of Neurological Disorders and Stroke grant NS29436 (M.P.N.), the University of Washington (A.E.C.), Fonds voor Wetenschappelijk Onderzoek (FWO) grant G.0580.06 (L.S.), and a FWO postdoctoral fellowship to J.H.

References

Ayali, A. and Harris-Warrick, R. M. (1999). Monoamine control of the pacemaker kernel and cycle frequency in the lobster pyloric network. *J. Neurosci.* **19**, 6712-6722.

Bartos, M. and Nusbaum, M. P. (1997). Intercircuit control of motor pattern modulation by presynaptic inhibition. *J. Neurosci.* **17**, 2247-2256.

Beenhakker, M. P. and Nusbaum, M. P. (2004). Mechanosensory activation of a motor circuit by coactivation of two projection neurons. *J. Neurosci.* **24**, 6741-6750.

Beenhakker, M. P., Blitz, D. M. and Nusbaum, M. P. (2004). Long-lasting activation of rhythmic neuronal activity by a novel mechanosensory system in the crustacean stomatogastric nervous system. *J. Neurophysiol.* **91**, 78-91.

Beenhakker, M. P., DeLong, N. D., Saideman, S. R., Nadim, F. and Nusbaum, M. P. (2005). Proprioceptor regulation of motor circuit activity by presynaptic inhibition of a modulatory projection neuron. *J. Neurosci.* **25**, 8794-8806.

Billimoria, C. P., Li, L. and Marder, E. (2005). Profiling of neuropeptides released at the stomatogastric ganglion of the crab, *Cancer borealis* with mass spectrometry. *J. Neurochem.* **95**, 191-199.

Birmingham, J. T., Billimoria, C. P., DeKlotz, T. R., Stewart, R. A. and Marder, E. (2003). Differential and history-dependent modulation of a stretch receptor in the stomatogastric system of the crab, *Cancer borealis. J. Neurophysiol.* **90**, 3608-3616.

Blackburn, M. B., Wagner, R. M., Shabanowitz, J., Kochansky, J. P., Hunt, D. F. and Raina, A. K. (1995). The isolation and identification of three diuretic kinins from the abdominal ventral nerve cord of adult *Helicoverpa zea*. *J. Insect Physiol.* **41**, 723-730.

Blitz, D. M. and Nusbaum, M. P. (1997). Motor pattern selection via inhibition of parallel pathways. *J. Neurosci.* **17**, 4965-4975.

Blitz, D. M., Christie, A. E., Marder, E. and Nusbaum, M. P. (1995). Distribution and effects of tachykinin-like peptides in the stomatogastric nervous system of the crab, *Cancer borealis*. *J. Comp. Neurol.* **354**, 282-294.

Blitz, D. M., Beenhakker, M. P. and Nusbaum, M. P. (2004). Different sensory systems share projection neurons but elicit distinct motor patterns. *J. Neurosci.* **24**, 11381-11390.

Christie, A. E., Lundquist, C. T., Nässel, D. R. and Nusbaum, M. P. (1997). Two novel tachykinin-related peptides from the nervous system of the crab *Cancer borealis*. *J. Exp. Biol.* **200**, 2279-2294.

Coast, G. M. (1998). The influence of neuropeptides on Malpighian tubule writhing and its significance for excretion. *Peptides* **19**, 469-480.

Coleman, M. J. and Nusbaum, M. P. (1994). Functional consequences of compartmentalization of synaptic input. *J. Neurosci.* **14**, 6544-6552.

Coleman, M. J., Konstart, P. H., Rothman, B. S. and Nusbaum, M. P. (1994). Neuropeptide degradation produces functional inactivation in the crustacean nervous system. *J. Neurosci.* **14**, 6205-6216.

Cox, K. J. A., Tensen, C. P., Van der Schors, R. C., Li, K. W., van Heerikhuizen, H., Vreugdenhil, E., Geraerts, W. P. M. and Burke, J. F. (1997). Cloning, characterization, and expression of a G-protein-coupled receptor from *Lymnaea stagnalis* and identification of a leucokinin-like peptide, PSFHSWSamide, as its endogenous ligand. *J. Neurosci.* **17**, 1197-1205.

Eisen, J. S. and Marder, E. (1982). Mechanisms underlying pattern generation in lobster stomatogastric ganglion as determined by selective inactivation of identified neurons. III. Synaptic connections of electrically coupled pyloric neurons. *J. Neurophysiol.* **48**, 1392-1415.

Fu, Q., Kutz, K. K., Schmidt, J. J. and Hsu, Y. A., Messinger, D. I., Cain, S. D., de la Iglesia, H. O., Christie, A. E. and Li, L. (2005). Hormone complement of the *Cancer productus* sinus gland and pericardial organ: an anatomical and mass spectrometric investigation. *J. Comp. Neurol.* **493**, 607-626.

Gäde, G. (2004). Regulation of intermediary metabolism and water balance of insects by neuropeptides. *Annu. Rev. Entomol.* **49**, 93-113.

Harris-Warrick, R. M., Marder, E., Selverston, A. I. and Moulins, M. (1992). *Dynamic Biological Networks: The Stomatogastric Nervous System*. Cambridge, MA: MIT Press.

Hayes, T. K., Pannabecker, T. L., Hinckley, D. J., Holman, G. M., Nachman, R. J., Petzel, D. H. and Beyenbach, K. W. (1989). Leucokinins, a new family of ion transport stimulators and inhibitors in insect Malpighian tubules. *Life Sci.* **44**, 1259-1266.

Hayes, T. K., Holman, G. M., Pannabecker, T. L., Wright, M. S., Strey, A. A., Nachman, R. J., Hoel, D. F., Olson, J. K. and Beyenbach, K. W. (1994). Culekinin depolarizing peptide: a mosquito leucokinin-like peptide that influences insect Malpighian tubule ion transport. *Regul. Pept.* **52**, 235-248.

Hertzberg, S. R., Li, L., Torfs, P., Schoofs, L., Marder, E. and Nusbaum, M. P. (2002). Pevkinin peptide actions in the stomatogastric ganglion. *Soc. Neurosci. Abstr.* **2002**, 270.18.

Holman, G. M., Cook, B. J. and Nachman, R. J. (1986). Isolation, primary structure and synthesis of two neuropeptides from *Leucophaea maderae*. *Comp. Biochem. Physiol.* **84C**, 271-276.

Holman, G. M., Nachman, R. J. and Wright, M. S. (1990). Insect neuropeptides. *Annu. Rev. Entomol.* **35**, 201-217.

Hooper, S. L. and Marder, E. (1987). Modulation of the lobster pyloric rhythm by the peptide proctolin. *J. Neurosci.* **7**, 2097-2112.

Huybrechts, J., Nusbaum, M. P., Vanden Bosch, L., Baggerman, G., De Loof, A. and Schoofs, L. (2003). Neuropeptidomic analysis of the brain and thoracic ganglion from the Jonah crab, *Cancer borealis*. *Biochem. Biophys. Res. Commun.* **308**, 535-544.

Jorge-Rivera, J. C. and Marder, E. (1996). TNRNFLRFamide and SDRNFLRFamide modulate muscles of the stomatogastric system of the crab *Cancer borealis*. *J. Comp. Physiol. A* **179**, 741-751.

Jorge-Rivera, J. C., Sen, K., Birmingham, J. T., Abbott, L. F. and Marder, E. (1998). Temporal dynamics of convergent modulation at a crustacean neuromuscular junction. *J. Neurophysiol.* **80**, 2559-2570.

Katz, P. S. and Harris-Warrick, R. M. (1989). Serotonergic/cholinergic muscle receptor cells in the crab stomatogastric nervous system. II. Rapid nicotinic and prolonged modulatory effects on neurons in the stomatogastric ganglion. *J. Neurophysiol.* **62**, 571-581.

Kiehn, O. and Harris-Warrick, R. M. (1992). Serotonergic stretch receptors induce plateau properties in a crustacean motor neuron by a dual-conductance mechanism. *J. Neurophysiol.* **68**, 485-495.

Kilman, V. L. and Marder, E. (1996). Ultrastructure of the stomatogastric ganglion neuropil of the crab, *Cancer borealis*. *J. Comp. Neurol.* **374**, 362-375.

Marder, E. and Thirumalai, V. (2002). Cellular, synaptic and network effects of neuromodulation. *Neural Netw.* **15**, 479-493.

Marder, E., Bucher, D., Schulz, D. J. and Taylor, A. L. (2005). Invertebrate central pattern generation moves along. *Curr. Biol.* **15**, R685-R699.

Messinger, D. I., Kutz, K. K., Le, T., Verley, D. R., Hsu, Y. W., Ngo, C. T., Cain, S. D., Birmingham, J. T., Li, L. and Christie, A. E. (2005). Identification and characterization of a tachykinin-containing neuroendocrine organ in the commissural ganglion of the crab *Cancer productus*. *J. Exp. Biol.* **208**, 3303-3319.

Miller, J. P. and Selverston, A. I. (1982). Mechanisms underlying pattern generation in lobster stomatogastric ganglion as determined by selective inactivation of identified neurons. II. Oscillatory properties of pyloric neurons. *J. Neurophysiol.* **48**, 1378-1391.

Nässel, D. R. (2002). Neuropeptides in the nervous system of *Drosophila* and other insects: multiple roles as neuromodulators and neurohormones. *Prog. Neurobiol.* **68**, 1-84.

Nässel, D. R., Cantera, R. and Karlsson, A. (1992). Neurons in the cockroach nervous system reacting with antisera to the neuropeptide leucokinin I. *J. Comp. Neurol.* **322**, 45-67.

Nieto, J., Veelaert, D., Derua, R., Waelkens, E., Cerstiaens, A., Coast, G., Devreese, B., Van Beeumen, J., Calderon, J., De Loof, A. et al. (1998). Identification of one tachykinin- and two kinin-related peptides in the brain of the white shrimp, *Penaeus vannamei*. *Biochem. Biophys. Res. Commun.* **248**, 406-411.

Norris, B. J., Coleman, M. J. and Nusbaum, M. P. (1994). Recruitment of a projection neuron determines gastric mill motor pattern selection in the stomatogastric nervous system of the crab, *Cancer borealis*. *J. Neurophysiol.* **72**, 1451-1463.

Nusbaum, M. P. and Beenhakker, M. P. (2002). A small-systems approach to motor pattern generation. *Nature* **417**, 343-350.

Nusbaum, M. P. and Marder, E. (1988). A neuronal role for a crustacean red pigment concentrating hormone-like peptide: neuromodulation of the pyloric rhythm in the crab, *Cancer borealis*. *J. Exp. Biol.* **135**, 165-181.

Nusbaum, M. P., Weimann, J. M., Golowasch. J. and Marder, E. (1992). Presynaptic control of modulatory fibers by their neural network targets. *J. Neurosci.* **12**, 2706-2714.

Nusbaum, M. P., Blitz, D. M., Swensen, A. M., Wood, D. and Marder, E. (2001). The roles of co-transmission in neural network modulation. *Trends Neurosci.* **24**, 146-154.

Predel, R., Kellner, R., Rapus, J., Penzlin, H. and Gade, G. (1997). Isolation and structural elucidation of eight kinins from the retrocerebral complex of the American cockroach, *Periplanta americana*. *Regul. Pept.* **71**, 199-205.

Schoofs, L., Holman, G. M., Proost, P., Van Damme, J., Hayes, T. K. and De Loof, A. (1992). Locustakinin, a novel myotropic peptide from *Locusta migratoria*, isolation, primary structure and synthesis. *Regul. Pept.* **37**, 49-57.

Skiebe, P. (2001). Neuropeptides are ubiquitous chemical mediators: using the stomatogastric nervous system as a model system. *J. Exp. Biol.* **204**, 2035-2048.

Stein, W., Eberle, C. C. and Hedrich, U. B. S. (2005). Motor pattern selection by nitric oxide in the stomatogastric nervous system of the crab. *Eur. J. Neurosci.* **21**, 2767-2781.

Te Brugge, V. A. and Orchard, I. (2002). Evidence for CRF-like and kinin-like peptides as neurohormones in the blood-feeding bug, *Rhodnius prolixus*. *Peptides* **23**, 1967-1979.

Te Brugge, V. A., Schooley, D. A. and Orchard, I. (2002). The biological activity of diuretic factors in *Rhodnius prolixus*. *Peptides* **23**, 671-681.

Terhzaz, S., O'Connell, F. C., Pollock, V. P., Kean, L., Davies, S. A., Veenstra, J. A. and Dow, J. A. (1999). Isolation and characterization of a leucokinin-like peptide of *Drosophila melanogaster*. *J. Exp. Biol.* **202**, 3667-3676.

Thirumalai, V., Prinz, A. A., Johnson, C. D. and Marder, E. (2006). Red pigment concentrating hormone strongly enhances the strength of the feedback to the pyloric rhythm oscillator but has little effect on pyloric rhythm period. *J. Neurophysiol.* **95**, 1762-1770.

Torfs, P., Nieto, J., Veelaert, D., Boon, D., van de Water, G., Waelkens, E., Derua, R., Calderon, J., De Loof, A. and Schoofs, L. (1999). The kinin peptide family in invertebrates. *Ann. N. Y. Acad. Sci.* **897**, 361-373.

Veenstra, J. A. (1994). Isolation and identification of three leucokinins from the mosquito *Aedes aegypto*. *Biochem. Biophys. Res. Commun.* **202**, 715-719.

Weimann, J. M., Marder, E., Evans, B. and Calabrese, R. L. (1993). The effects of SDRNFLRFamide and TNRNFLRFamide on the motor patterns of the stomatogastric ganglion of the crab *Cancer borealis*. *J. Exp. Biol.* **181**, 1-26.

Wood, D. E. and Nusbaum, M. P. (2002). Extracellular peptidase activity tunes motor pattern modulation. *J. Neurosci.* **22**, 4185-4195.

Wood, D. E., Stein, W. and Nusbaum, M. P. (2000). Projection neurons with shared cotransmitters elicit different motor patterns from the same neural circuit. *J. Neurosci.* **20**, 8943-8953.

Wood, D. E., Manor, Y., Nadim, F. and Nusbaum, M. P. (2004). Intercircuit control via rhythmic regulation of projection neuron activity. *J. Neurosci.* **24**, 7455-7463.